High-Efficiency Defect-Based Photonic-Crystal Tapers Designed by a Genetic Algorithm

Andreas Håkansson, Pablo Sanchis, José Sánchez-Dehesa, and Javier Martí, *Member, IEEE*

***Abstract*—A method based on a genetic algorithm (GA) is used to design the optimum configuration of defects that when put within a photonic-crystal (PhC) taper improve the coupling efficiency between dielectric and PhC waveguides (WGs). This approach optimizes the whole configuration of defects simultaneously and, therefore, takes into account the correlation among the defects. Transmission efficiencies up to 94% have been predicted for a 3-μm-wide dielectric WG into a single-line-defect PhC-WG. This result significantly improves the transmission efficiency of the same PhC taper without defects. The influence on the coupling efficiency of the PhC taper length and geometry are also discussed.**

***Index Terms*—Coupling, genetic algorithms, inverse design, multiple scattering, optimization, photonic crystals, photonic integrated circuits.**

I. Introduction

In RECENT years, a large variety of functionalities based on photonic crystals (PhCs) have been reported, aiming at the realization of highly integrated photonic circuits [1]. There has also been a considerable progress in the fabrication processes. However, a great effort is still needed to resolve several issues to permit the definitive industrial deployment of PhC technology. Among them, the minimization of propagation losses and coupling losses between PhC circuits and external media, like fiber and dielectric waveguides (WGs), plays a crucial role. A large variety of coupling structures and techniques to minimize the coupling losses between PhC-WGs and dielectric WGs have been proposed in the last few years [2]–[7]. One of the most promising approaches are discrete PhC tapers made by producing defects at the entrance of the original PhC-WG [8]–[11].

A coupling technique based on properly inserting localized defects within a PhC taper was proposed and experimentally demonstrated by some of the authors [12]–[14] to improve the coupling efficiency between dielectric WGs and PhC-WGs. The optimum configuration of defects was designed by means of a heuristic optimization approach. However, this approach comes out inefficient; in addition, it could not lead to the best design when the required number of defects is increased.

Genetic algorithms (GAs) are one of the best approaches to solve complex problems with a large set of parameters. They have been employed to tackle different complex problems in PhC structures [15]–[19]. Thus, in the same spirit as in [13], a microgenetic algorithm (μGA) was recently used to design the optimum configuration of defects within a PhC taper [15]. The proposed defects were of unconventional shape, and they were placed out of the mirror plane of the PhC taper. However, only one type of PhC taper was analyzed, and no dependence on frequencies was reported [15].

In this paper, a GA have been used for properly designing the optimum configuration of defects considering PhC tapers with different lengths and geometries in order to achieve the highest transmission efficiency in a broad frequency range. One of the most popular GAs used in combination with multiple scattering theory (MST) to evaluate the transmission across the PhC structures has been considered. This GA-MST inverse design tool has previously used by some of the authors to solve equivalent problems in photonics [18], [19]. The same tool is used here with the reservation that the GA is implemented with Gray codes to improve the performance with real-valued parameters. In comparison with [15], where only one type of PhC taper was analyzed and no dependence on frequency was reported, here, we report a comprehensive study of different PhC tapers and analysis of the influence on the coupling efficiency of the correlation between defects, the PhC taper length, the PhC taper geometry, and the frequency of optimization are presented.

The paper is structured as follows. In Section II, the design of the optimum configuration of defects producing maximum transmission at a given frequency is initially carried out by calculating all the possible solutions in terms of the radius and relative position of the defects placed within the PhC taper. It will be discussed how this approach is impractical for many cases of interest and, therefore, in Section III, a design approach based on GA-MST is proposed and applied. Particularly, the parameters of defects placed in several PhC tapers with different geometries are optimized to predict the highest transmission efficiency. Finally, conclusions are given in Section IV.

II. Defects Configuration Determined by a Calculation of the Full Set of Solutions

The considered PhC is formed by a two-dimensional (2-D) hexagonal lattice of dielectric cylindrical rods of silicon (Si) embedded in a silica (SiO_2) background. The radius R of the rods is $0.2a$, a being the lattice constant. A PhC structure similar to the one studied here was recently fabricated with a square-lattice configuration [20]. A single line of defects in the PhC made the PhC-WG to where a 3-μm-wide dielectric WG

Manuscript received January 24, 2005; revised June 28, 2005. This work was partially funded by the Spanish Ministry of Education and Science (MEC) under grants with references TIC2002-01553 and TEC2004-03545, by the Comunidad Autónoma de Madrid under grant with reference GR/MAT/0729/2004 and by the Accion Estrategica Nano with reference NAN2004-08843-C05-04. The Ph.D. work of P. Sanchis was funded by a Spanish MEC.

The authors are with the Nanophotonics Technology Center, Universidad Politécnica de Valencia, Valencia 46022, Spain (e-mail: andreas@ntc.upv.es; pabsanki@ntc.upv.es; jsdehesa@upvnet.upv.es; jmarti@dcom.upv.es).

Digital Object Identifier 10.1109/JLT.2005.857760

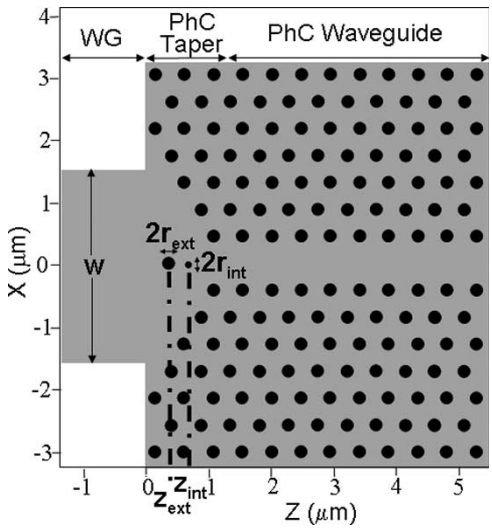

Fig. 1. Schematic of the coupling structure under analysis. The PhC taper, which has a length of $2a$ (a being the lattice constant of the PhC), is used to facilitate the coupling of light from a 3-μm-wide (w in figure) silica dielectric WG into the PhC-WG. $r_{\rm ext}$ and $r_{\rm int}$ ($z_{\rm ext}$ and $z_{\rm int}$) label the radii (position) of the external and internal cylinders, respectively, placed within the PhC taper.

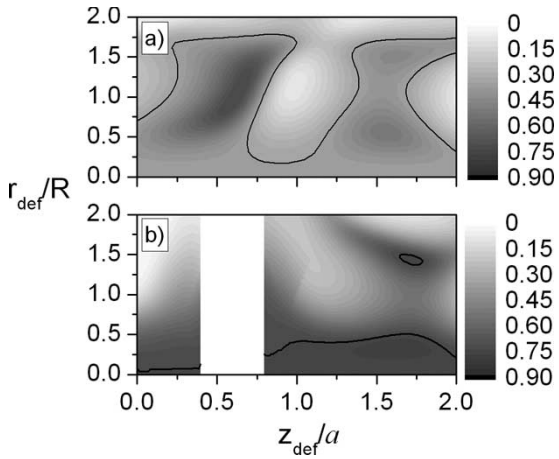

Fig. 2. (a) Transmission map for the case of a single defect in the coupling structure shown in Fig. 1. The transmission efficiency is plot as a function of the normalized defect radius $r_{\rm def}/R$ (R being the radius of the rods of the PhC) and the relative position in the z-axis within the $2a$-long PhC taper $z_{\rm def}/a$. (b) Transmission map for the case of two defects. One defect with radius $r_{\rm def} = 1.03R$ is fixed at position $z_{\rm def} = 0.63a$ within the PhC taper. The map shows the transmission efficiency as a function of the radius and position of the second defect. The white area defines the region of overlap of the two defects, and within that region, the transmission cannot be calculated. The black lines in the two figures separate the regions for which a transmission improvement is achieved (see text).

is coupled. On the one hand, the PhC structure has a bandgap for the transverse magnetic (TM) modes [electric field pointed out of the plane E_y(x, z)] defined in the normalized frequency range 0.266–0.359 (a/λ). On the other hand, the PhC-WG has a single mode with bandwidth in the range 0.274–0.347 (a/λ).

Fig. 1 schematically shows the coupling configuration that is analyzed in this section. This coupling structure consists of two cylindrical defects with radius $r_{\rm ext}$ and $r_{\rm int}$, respectively, placed within the PhC taper. The same configuration was analyzed in a previous work and a maximum transmission of 84% was predicted for the optimized configuration of defects [13]. The optimum configuration of defects was obtained by means of a heuristic approach based on first deciding the number of defects, and their relative position, that should be placed into the PhC taper and then optimizing the radius of each defect [13].

Here, the optimum two-defect configuration is recalculated by studying all the possible solutions in terms of the radius and relative position of the defects placed at the entrance of the PhC-WG. This calculation becomes feasible by using an MST, previously used by some of the authors [21]. The MST significantly reduces the computational time required to calculate the transmission power through any given 2-D PhC structure with respect to the finite-difference time-domain (FDTD) method, which was the numerical technique employed in [13]. However, for the sake of comparison with earlier works, the transmission spectra of the resulting optimized PhC structures have been calculated throughout this paper by using the FDTD method. A good agreement was always found between the two simulation methods.

For the case of a single defect within the PhC taper, Fig. 2(a) shows the transmission efficiency as a function of the defect radius $r_{\rm def}$ and the relative position in the z-axis $z_{\rm def}$ at the normalized frequency of 0.30 (a/λ). It can be seen that the there is a dominant maximum of 79% for a radius of $r_{\rm def} = 1.03R$ and at a position of $z_{\rm def} = 0.63a$. The black line in Fig. 2(a) separates the region of parameters where the transmission is enhanced with respect to the corresponding PhC taper without defects. The large range of parameters producing transmission improvement concludes that a single-defect configuration is a very good tool to enhance the power transmission into the PhC-WG, and, besides, it is noticeable that the enhancement is very robust against possible errors in the position and radius of the defect.

After fixing the best defect with these parameters, the transmission map has been recalculated for the case of a second defect put within the taper (see Fig. 1). Fig. 2(b) shows the resulting map, which indicates that the transmission is improved up to 87% when a defect with parameters $(r_{\rm int}, z_{\rm int}) = (0.34R, 1.63a)$ is added into the taper. The parameters of the two-defect configuration are similar to those reported in [13] and, therefore, the transmission has only been slightly improved. The black line in Fig. 2(b) defines the region of parameters where the second defect has to be placed in order to get transmission enhancement with respect to the single-defect configuration. Now, it can be noticed that the region of parameter producing transmission enhancement is quite small and, in addition, that the enhancement will be more sensible to possible errors of fabrication in the position and radius of this additional defect. Fig. 3 shows the transmission efficiency as a function of frequency for the PhC taper without defects (dashed line) in comparison with the 2 two-defect configurations described above.

Let us remark that the calculation of all possible configurations for the one-defect problem guarantees that the true optimum parameters have been obtained. This calculation has been made possible, because the computational time needed to calculate the map shown in Fig. 2(a) is relatively short by using MST. Notice that the total number of possible solutions

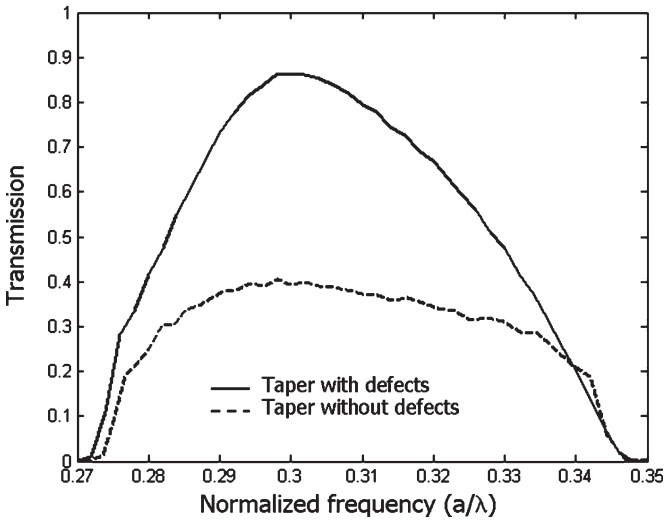

Fig. 3. Transmission efficiency as a function of the normalized frequency for the PhC taper shown in Fig. 1. The efficiency of the PhC taper without defects (dotted line) is compared with the one containing two defects whose parameters are optimized with a GA at the normalized frequency of 0.30 (a/λ).

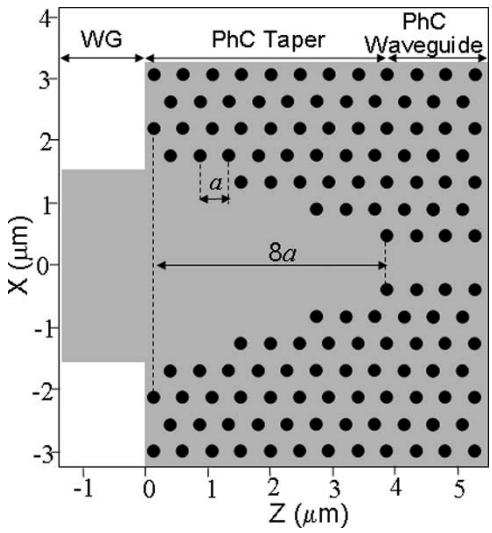

Fig. 4. Schematic of the coupling structure consisting of an $8a$-long PhC taper that couples a 3-μm-wide dielectric WG into the PhC-WG.

is $N = (2a/\Delta z_{\rm def})/(2R/\Delta r_{\rm def})$, where $\Delta z_{\rm def}$ and $\Delta r_{\rm def}$ are the steps related to the position and radius of the defect, respectively. Thus, for steps values of $\Delta z_{\rm def} = 0.031a$ and $\Delta r_{\rm def} = 0.0625R$, the total number of configurations is $64 \times 32 = 2048$, which can be calculated using a Pentium IV personal home computer in less than 12 h. However, if one wants to explore the full set of solutions for the two-defect case, the number N would increase up to 2 096 128. This number is about 1000 times larger than for the single-defect case and implies a calculation time of about 1.5 years. Because of this computational effort, the map in Fig. 2(b) has been calculated under the approach of fixing one of the defects at the position where a single-defect configuration maximizes the transmission [see Fig. 2(a)]. Fortunately, the correlation between defects is not very large for this $2a$-long PhC taper. This lack of correlation is observed in Fig. 2(a) and (b) since the maximum transmission obtained by putting two defects at the maxima in Fig. 2(a) [respectively, at $(r_{\rm ext}, z_{\rm ext}) = (1.03R, 0.63a)$ and $(r_{\rm int}, z_{\rm int}) = (0.58R, 1.56a)$] does not differ much from the one obtained when the second defect is put at the maximum obtained in Fig. 2(b); that is, at $(r'_{\rm int}, z'_{\rm int}) = (0.34R, 1.63a)$.

Unfortunately, the correlation between defects becomes an important issue either when the PhC taper is made longer or when the number of the defects within the taper is greater than two. In other words, the defect correlation could be an important drawback in order to determine the true maximum transmission efficiency. For example, for an $8a$-long PhC taper like the one shown in Fig. 4, the search for the optimum parameters of the second defect is conditioned by the parameters chosen for the first defect. This phenomenon is clearly shown in the transmission maps represented in Fig. 5. In those maps, the black lines separate the regions where an improvement of the transmission is achieved with respect to the case without defects [in Fig. 5(a)] or for the single-defect case [in Fig. 5(b) and (c)]. Now, the importance of the correlation is observed. A sensible difference between transmissions is obtained depending on

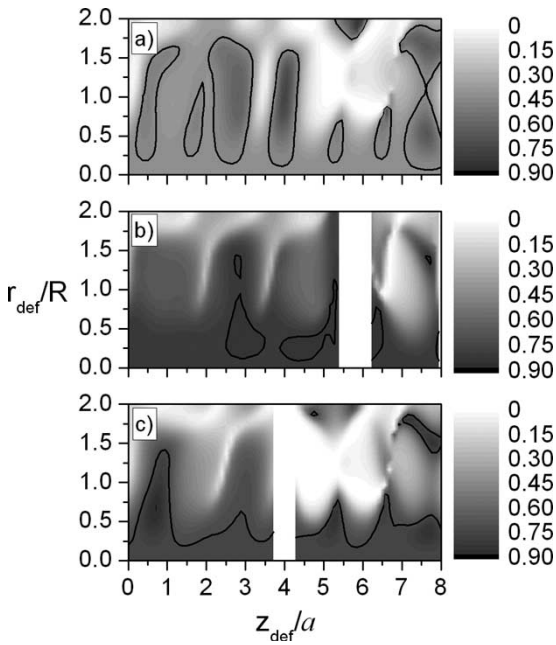

Fig. 5. (a) Transmission map for the case of a single defect within the structure shown in Fig. 4. The transmission T is plotted as a function of the defect radius $r_{\rm def}$ and its position $z_{\rm def}$ in the z-axis. (b) Transmission map for the case with two defects. The first defect is fixed with parameters determined by the first maximum in (a); i.e., with values $(r_1, z_1) = (1.88R, 5.74a)$ fixed. The map reports the transmission as a function of the radius and position of the second defect. (c) Transmission map for the case in which the first defect is fixed with parameters $(r_1, z_1) = (1.09R, 0.65a)$, which corresponds to the second maximum in (a). White areas define the regions of parameters where T cannot be calculated because of the overlap between defects. The black lines in the three figures separate the regions for which a transmission improvement is achieved (see text).

where the first defect is placed. Fig. 5(b) shows the transmission for the second defect, if the parameters for the first defect are taken from the global maximum in Fig. 5(a) (as was done for the $2a$-long taper). The best result for the two-defect configuration corresponds to the global maximum in Fig. 5(b) and equals a

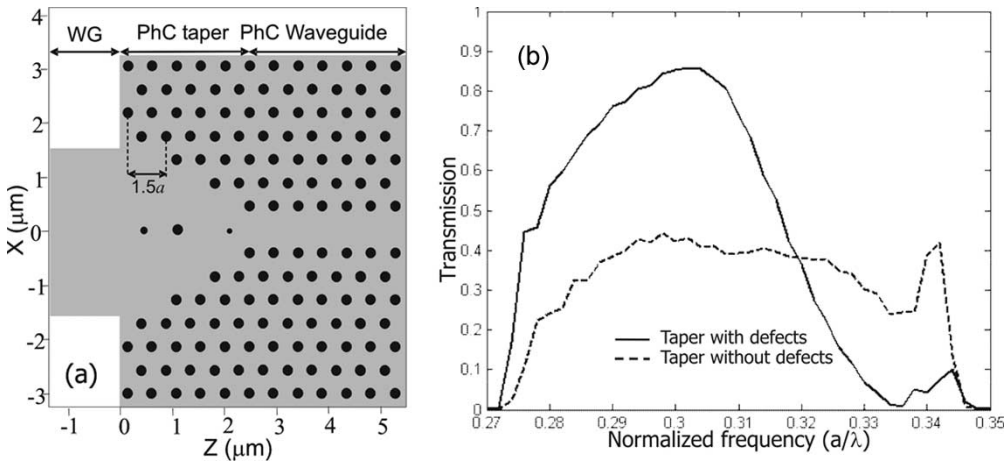

Fig. 6. (a) Schematic of the $5a$-long PhC taper that is made of discrete steps having a length of $1.5a$. (b) Transmission efficiency as a function of the frequency using the PhC taper without and with the optimized three-defect configuration. The parameters of the defects are reported in Table I, and they were obtained to get a maximum transmission at the frequency of 0.30 (a/λ).

transmission of 83%. Fig. 5(c) shows the second defect dependency for using, not the best, but the second best solution from Fig. 5(a). Surprisingly, the global maximum in Fig. 5(c) predicts a coupling efficiency of 90%, outperforming the earlier 83%.

The discussion above lets us to conclude that though high transmission efficiency is achieved by following the previous approach, alternative efficient approaches that simultaneously optimize the whole configuration of defects would be more appropriate in order to get the defect parameters giving the true maximum of power transmission into the PhC-WG.

III. Defects Configuration Determined by a GA-MST Tool

Here, a design approach based on a GA-MST tool of design that has been successfully employed by some of the authors in several optimization problems [18], [19], [22], [23] is applied to get the parameters of the defects that introduced within the PhC taper produces the maximum power transmission into the PhC-WG.

First, the parameters of two defects within the $2a$-long PhC taper shown in Fig. 1 were calculated. The optimum parameters obtained are $(r_{\rm int}, z_{\rm int}) = (0.38R, 1.48a)$ and $(r_{\rm ext}, z_{\rm ext}) = (0.84R, 0.6a)$. These parameters are somewhat different to those previously reported, but the transmission efficiency is not significantly improved. The optimization was also carried out for a three-defect configuration, but the transmission efficiency was, once again, not substantially improved. However, just as occurs in conventional dielectric tapers, the transmission efficiency depends on the length of the PhC taper [10]. Below, it is shown how higher transmission efficiencies could be achieved by using a PhC taper longer than the previously considered.

A. Optimization of the PhC Taper Length

The structure shown in Fig. 6(a), which is named as a $5a$-long PhC taper, has firstly been considered. It has a staircase-like profile with $1.5a$-long steps. The optimum transmission is searched considering configurations of one, two, three, and four defects within the taper. On the one hand, the case of four-defect configuration resulted in a transmission efficiency only 1% higher than the three-defect case but in a much narrower frequency band. On the other hand, the one- and two-defect configurations gave lower efficiencies than the three-defect configurations. Therefore, the three-defect case is considered as the best solution and will be reported here. The optimum parameters of the defects (i.e., radii and positions, respectively) producing maximum transmission at the optimized frequency of 0.30 (a/λ) are reported in Table I. The transmission efficiency achieved with these three-defect configuration is 86%, which does not improve the 87% achieved with the $2a$-long PhC taper depicted in Fig. 1. The transmission as a function of the frequency is shown in Fig. 6(b) for the optimized configuration (continuous line) and is compared with the one free of defects (dashed line). It is noticeable in Fig. 6(b) how a broad bandwidth with transmission efficiencies above 80% is achieved for the PhC taper with three defects.

TABLE I
Optimum Radii and Positions of the Three-Defect Configuration Obtained by Means of the GA-MST Optimization Tool That Maximize the Transmission Across the PhC Structure Shown in Fig. 6(a) at the Frequency of $0.3(a/\lambda)$

	Position	Radius
Defect #1	$1.77a$	$0.38R$
Defect #2	$2.09a$	$1.03R$
Defect #3	$4.68a$	$0.64R$

Since the transmission in the $5a$-long PhC taper has not effectively improved with respect to the shorter taper, a longer PhC taper, as the one shown in Fig. 7(a), has been considered. In this case, the taper is made of discrete steps having a length of $2.5a$. As before, the best results were obtained for a three-defect configuration. The optimum radii and positions of the defects calculated at the normalized frequency of 0.30 (a/λ) are reported in Table II. A transmission efficiency up to 94% is obtained in this case, which improves the transmission efficiency achieved with the shorter tapers previously studied. The transmission spectrum is shown in Fig. 7(b) for this PhC

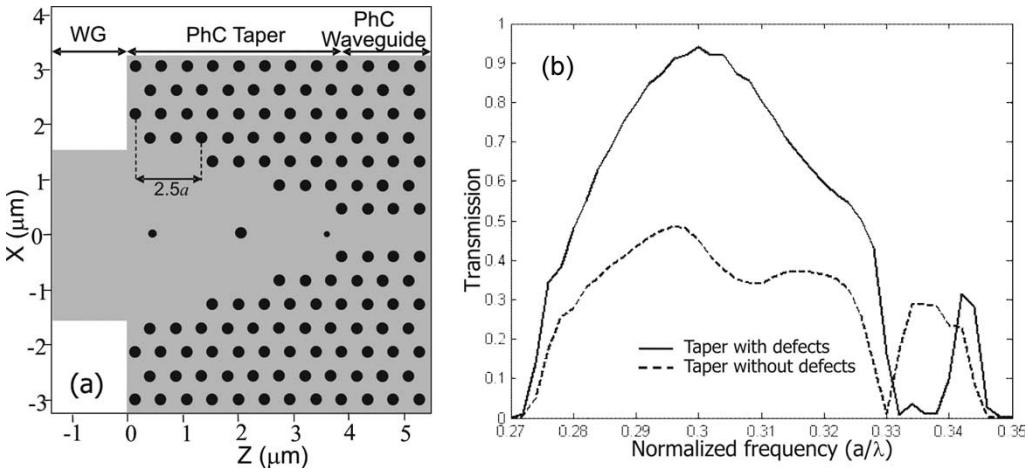

Fig. 7. (a) Schematic of the longer PhC taper that is made of discrete steps having a length of $2.5a$. (b) Transmission efficiency as a function of the frequency using the PhC taper without and with the optimized three-defect configuration. The parameters of the defects are reported in Table II, and they were obtained to get a maximum transmission at the frequency of 0.30 (a/λ).

TABLE II
OPTIMUM RADII AND POSITIONS OF THE THREE-DEFECT CONFIGURATION OBTAINED BY MEANS OF THE GA-MST OPTIMIZATION TOOL FOR THE $8a$-LONG PhC TAPER [SEE FIG. 7(a)] AT THREE DIFFERENT FREQUENCIES OF OPTIMIZATION (IN NORMALIZED UNITS)

	f=0.30		f=0.32		f=0.335	
	Position	Radius	Position	Radius	Position	Radius
Defect #1	0.76a	0.45R	1.01a	0.45R	2.54a	0.45R
Defect #2	2.92a	0.77R	2.92a	0.77R	3.05a	0.71R
Defect #3	7.49a	0.45R	6.22a	0.77R	7.62a	1.22R

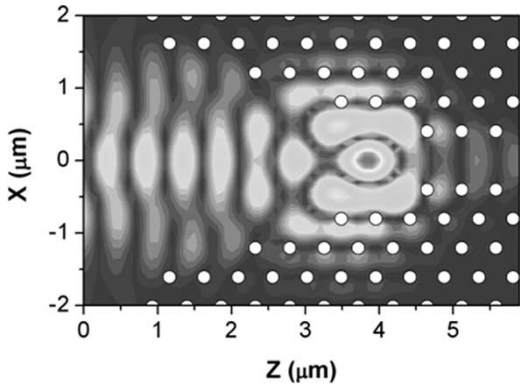

Fig. 8. Modulus of the electric field at a normalized frequency of 0.329 (a/λ) for the structure shown in Fig. 7(a) and without considering defects within the PhC taper.

taper with the optimized three-defect configuration (continuous line) and is compared with the free-defect configuration (dashed line). A broad bandwidth with transmission efficiencies above 80% is obtained for this PhC taper. However, the transmission at high frequencies presents a bad behavior in both configurations. Particularly, the transmission for this PhC taper without defects sharply drops at the normalized frequency of 0.329; this behavior is also observed in the three-defect PhC taper but at slightly higher frequencies.

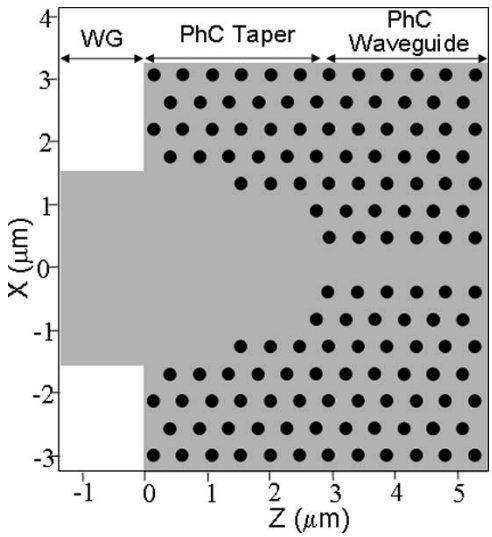

Fig. 9. Schematic diagram of the $6a$-long modified PhC taper proposed to avoid the excitation of the resonant mode shown in Fig. 8.

B. Modification of the PhC Taper Geometry

In order to analyze more in-depth this effect, the modulus of the electric field, $|E_y(x,z)|$ has been obtained for the $8a$-long PhC taper without defects at 0.329 (a/λ), the frequency at which the transmission suddenly drops. The plot, which is shown in Fig. 8, indicates that a long-live resonant mode is excited near the end of the PhC taper, thus, strongly reducing the power transmitted into the PhC-WG. The physical origin of this resonant behavior is out of the scope of the present work. It could be explained by using coupled mode theory [24], but details will be given in a further publication.

In order to avoid the excitation of the resonant mode, we have suppressed the section of the taper closer to the PhC-WG. The resulting taper that we named as a $6a$-long modified taper is depicted in Fig. 9. The spectrum transmission of this new taper without defects is shown in Fig. 10, and it is compared with those presenting the anomalous behavior at high frequencies. It

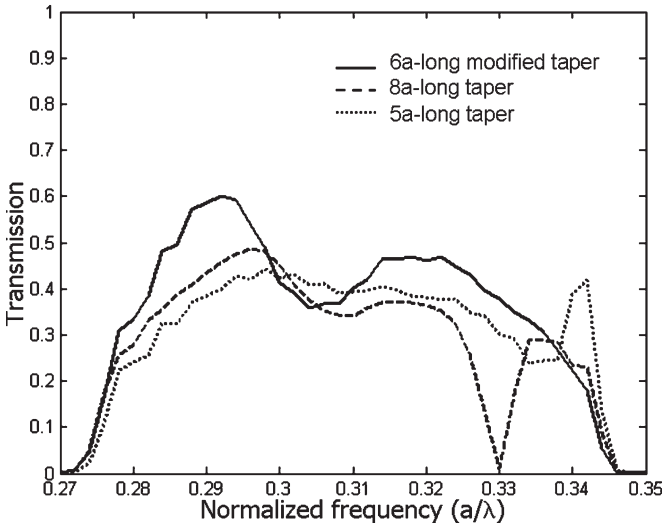

Fig. 10. Transmission efficiency as a function of the normalized frequency using the $6a$-long modified PhC taper (see Fig. 9), and the $5a$- and $8a$-long PhC tapers shown in Fig. 6(a) and 7(a), respectively. In all cases, no defects were placed within the corresponding PhC tapers.

TABLE III
OPTIMUM RADII AND POSITIONS OF THE THREE-DEFECT CONFIGURATION OBTAINED BY MEANS OF THE GA-MST OPTIMIZATION TOOL FOR THE $6a$-LONG MODIFIED PHC TAPER [SEE FIG. 9] AT THREE DIFFERENT FREQUENCIES OF OPTIMIZATION (IN NORMALIZED UNITS)

	f=0.30		f=0.32		f=0.335	
	Position	Radius	Position	Radius	Position	Radius
Defect #1	$0.57a$	$0.71R$	$1.14a$	$0.64R$	$0.00a$	$0.77R$
Defect #2	$2.95a$	$0.64R$	$2.85a$	$0.64R$	$4.86a$	$0.45R$
Defect #3	$5.62a$	$0.71R$	$5.52a$	$1.16R$	$5.71a$	$1.03R$

can be seen that the transmission does not show the drop at high frequencies, because the localized mode has been removed.

The close-to-zero transmission observed at frequencies around 0.335 (a/λ) for the $5a$-long and $8a$-long PhC tapers with three defects inside can also be explained by a similar resonant effect. Therefore, the optimization of a three-defect configuration at the frequency of 0.30 (a/λ) has also been carried out for the so-called $6a$-long modified PhC taper. The optimized parameters are given in Table III, and the transmission spectrum is shown in Fig. 11, where a comparison with the one obtained for the $8a$-long PhC taper is depicted. The maximum transmission efficiency is 92%, however, in this case, the transmission is not degraded at frequencies around 0.33 (a/λ). This result confirms that the last section of the $8a$-long PhC taper has a large influence on the coupling efficiency at high frequencies. The suppression of this section in the $6a$-long modified PhC taper has produced the transmission enhancement at those frequencies.

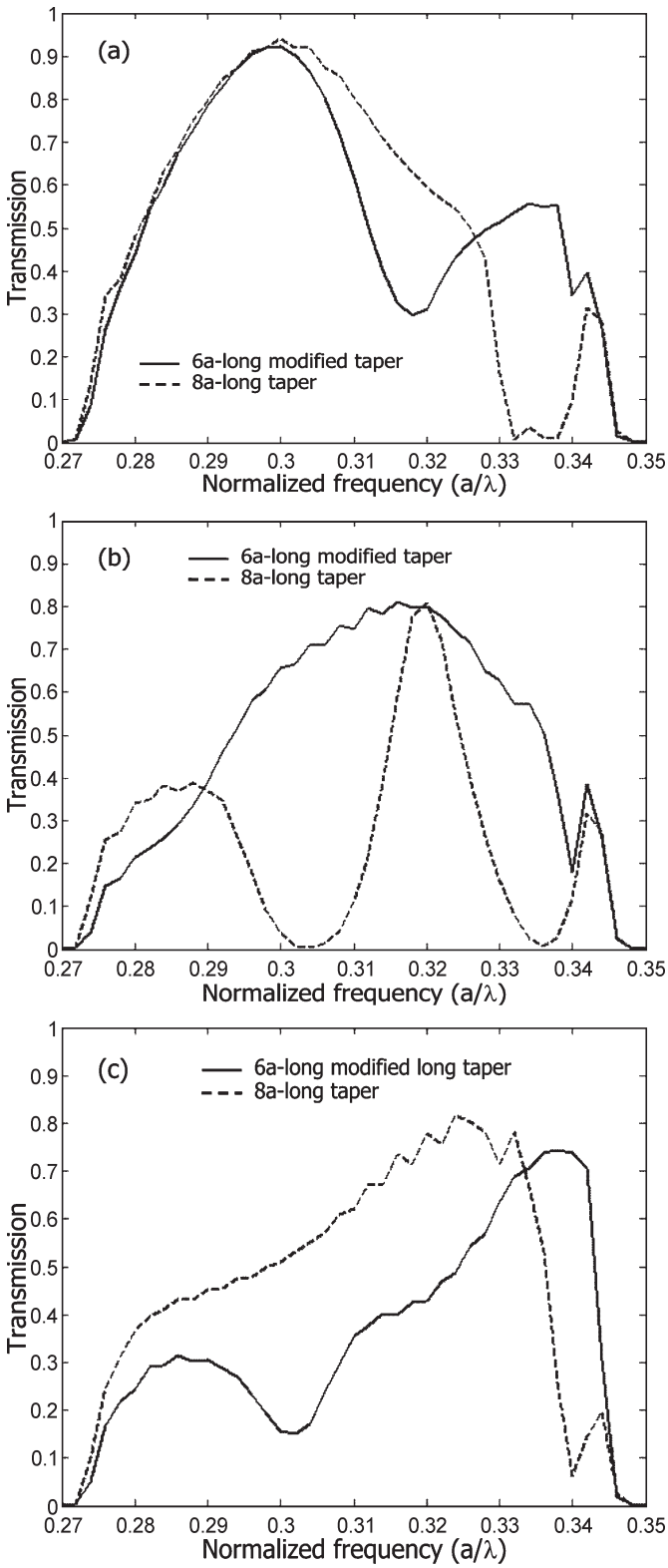

Fig. 11. Transmission efficiency as a function of the normalized frequency using the $8a$-long PhC taper shown in Fig. 7(a) and the $6a$-long modified PhC taper shown in Fig. 9, each one with its corresponding three-defect configuration optimized at the frequency of (a) 0.3 (a/λ), (b) 0.32 (a/λ), and (c) 0.335 (a/λ).

C. Coupling Dependence on the Frequency of Optimization

The transmission efficiency can be improved at any given frequency since defect parameters depend on the frequency used in the optimization process. To prove the usefulness of the proposed coupling technique, the optimization of the three-defect configuration has been repeated for the $8a$-long PhC taper at the frequencies of 0.32 (a/λ) and 0.335 (a/λ). The

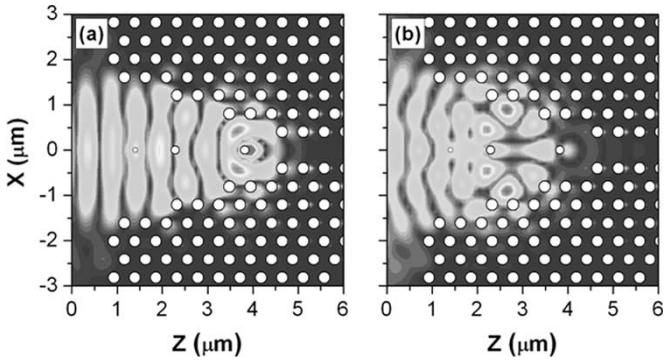

Fig. 12. Modulus of the electric field for the $8a$-long PhC taper at the normalized frequencies of (a) 0.303 (a/λ) and (b) 0.3355 (a/λ). The parameters of the three-defect configuration optimized at the normalized frequency of 0.32 (a/λ) (see Table II) are used within each PhC taper.

parameters are reported in Table II, and the corresponding transmission spectra are plotted as dashed lines in Fig. 11. Let us remark how the parameters of defect 3, which is located within the section of the taper closer to the PhC-WG, are the ones that differ more from the values obtained for the other two optimization frequencies. This result is expected since the coupling efficiency at frequencies around 0.33 (a/λ) is highly dependent on the thickness of the section closer to the PhC-WG. However, the more relevant feature in these spectra is the presence of drops in the transmission for certain frequencies. As discussed before, these drops are related to the existence of long life resonances now existing in the PhC taper with defects. As an example, Fig. 12 plots the map of the electric field modulus for the two resonances existing at the structure optimized at 0.32 (a/λ).

The optimization of the three-defect configuration and the calculation of the corresponding transmission spectra have also been carried out for the $6a$-long modified PhC taper (see Table III and Fig. 11). Now, the transmission spectra for this PhC taper does not present such abrupt drops, though regions of minimum transmission are still seen at different frequencies in the band. Furthermore, it can be seen in Fig. 11(c) that higher transmission efficiencies at frequencies closer to the band edge are achieved with respect to the $8a$-long PhC taper.

Finally, in regards with the $2a$-long PhC taper (see Fig. 1), which is the shortest taper studied, it is important to point out that no minimum transmission is found in the spectra (see Fig. 3) either in the PhC taper without defects or in the PhC taper with defects, because no localized states are built in the different sections that form the PhC taper.

IV. Conclusion

A coupling technique based on setting localized defects within a photonic-crystal (PhC) taper has been thoroughly analyzed. The optimum number of defects as well as their radii and position within the PhC taper need to be carefully designed depending on the size of the PhC taper. For small PhC tapers, the optimum parameters may be achieved by making a scan of all the possible solutions. However, this approach does not take into account the correlation among defects so it cannot lead to the best solution when a high number of defects are required. Therefore, in this case, the design of the optimum configuration of defects has been proposed based on a stochastic search algorithm, which is a genetic algorithm (GA), used in conjunction with a multiple scattering theory (MST) to calculate the transmission across the structures under study.

On the other hand, the influence of the PhC taper length on the coupling efficiency has also been analyzed. It has been found that resonant modes can be excited when the length of the PhC taper is increased, thus, degrading the coupling efficiency. However, these resonant modes can be avoided by carefully designing the PhC taper geometry. Furthermore, the transmission efficiency is maximized when the proposed coupling technique is used.

In summary, transmission efficiencies above 90% for coupling light from a 3-μm-wide dielectric waveguide (WG) into the PhC-WG have been demonstrated by using the proposed coupling technique. In all the different analyzed PhC tapers, the transmission efficiency was significantly improved with respect to the case of using the same PhC taper without defects.

References

[1] J. D. Joannopoulos, R. D. Meade, and N. J. Winn, *Photonic Crystals: Molding the Flow of Light*. Princeton, NJ: Princeton Univ. Press, Sep. 1995.

[2] Y. Xu, R. Lee, and A. Yariv, "Adiabatic coupling between conventional dielectric waveguides and waveguides with discrete translational symmetry," *Opt. Lett.*, vol. 25, no. 10, pp. 755–757, 2000.

[3] A. Mekis and J. D. Joannopoulos, "Tapered couplers for efficient interfacing between dielectric and PhC waveguides," *J. Lightw. Technol.*, vol. 19, no. 6, pp. 861–865, Jun. 2001.

[4] D. W. Prather, J. Murakowski, S. Shi, S. Venkataram, A. Sharkawy, C. Chen, and D. Pustai, "High-efficiency coupling structure for a single-line-defect photonic-crystal waveguide," *Opt. Lett.*, vol. 27, no. 18, pp. 1601–1603, 2002.

[5] P. E. Barclay, K. Srinivasan, M. Borselli, and O. Painter, "Experimental demonstration of evanescent coupling from optical fibre tapers to photonic crystal waveguides," *Electron. Lett.*, vol. 39, no. 11, pp. 842–844, May 2003.

[6] W. Kuang, C. Kim, A. Stapleton, and J. D. O'Brien, "Grating-assisted coupling of optical fibers and photonic crystal waveguides," *Opt. Lett.*, vol. 27, no. 18, pp. 1604–1606, 2002.

[7] A. Talneau, M. Agio, C. M. Soukoulis, M. Mulot, S. Anand, and P. Lalanne, "High-bandwidth transmission of an efficient photonic-crystal mode converter," *Opt. Lett.*, vol. 29, no. 15, pp. 1745–1747, 2004.

[8] P. Pottier, I. Ntakis, and R. M. De La Rue, "PhC continuous taper for low-loss direct coupling into 2D PhC channel waveguides and further device functionality," *Opt. Commun.*, vol. 223, no. 4–6, pp. 339–347, 2003.

[9] P. Bienstman, S. Assefa, S. G. Johnson, J. D. Joannopoulos, G. S. Petrich, and L. A. Kolodziejski, "Taper structures for coupling into PhC slab waveguides," *J. Opt. Soc. Amer. B, Opt. Phys.*, vol. 20, no. 9, pp. 1817–1821, 2003.

[10] T. D. Happ, M. Kamp, and A. Forchel, "PhC tapers for ultracompact mode conversion," *Opt. Lett.*, vol. 26, no. 14, pp. 1102–1104, 2001.

[11] M. Dinu, R. L. Willett, K. Baldwin, L. N. Pfeiffer, and K. W. West, "Waveguide tapers and waveguide bends in AlGaAs-based two-dimensional photonic crystals," *Appl. Phys. Lett.*, vol. 83, no. 22, pp. 4471–4473, 2003

[12] P. Sanchis, J. Martí, A. García, A. Martínez, and J. Blasco, "High efficiency coupling technique for planar photonic crystal waveguides," *Electron. Lett.*, vol. 38, no. 17, pp. 961–962, Aug. 2002.

[13] P. Sanchis, J. Martí, J. Blasco, A. Martínez, and A. García, "Mode matching technique for highly efficient coupling between dielectric waveguides and planar photonic crystal circuits," *Opt. Express*, vol. 10, no. 24, pp. 1391–1397, 2002.

[14] P. Sanchis, J. García, J. Martí, W. Bogaerts, P. Dumon, D. Taillaert, R. Baets, V. Wiaux, J. Wouters, and S. Beckx, "Experimental demonstration of high coupling efficiency between wide ridge waveguides and single-mode photonic crystal waveguides," *IEEE Photon. Technol. Lett.*, vol. 16, no. 10, pp. 2272–2274, Oct. 2004.
[15] J. Jiang, J. Cai, G. P. Nordin, and L. Li, "Parallel microgenetic algorithm design for photonic crystal and waveguide structures," *Opt. Lett.*, vol. 28, no. 23, pp. 2381–2383, 2003.
[16] P. Borel, A. Harpoth, L. Frandsen, and M. Kristensen, "Topology optimization and fabrication of photonic crystal structures," *Opt. Express*, vol. 12, no. 9, pp. 1996–2001, 2004.
[17] L. Shen, Z. Ye, and S. He, "Design of two-dimensional photonic crystals with large absolute band gaps using a genetic algorithm," *Phys. Rev. B, Condens. Matter*, vol. 68, no. 3, p. 035109, 2003.
[18] L. Sanchis, A. Håkanson, D. López-Zanón, J. Bravo-Abad, and J. Sánchez-Dehesa, "Integrated optical devices design by genetic algorithm," *Appl. Phys. Lett.*, vol. 84, no. 22, pp. 4460–4462, 2004.
[19] A. Håkanson, J. Sánchez-Dehesa, and L. Sanchis, "Inverse design of photonic crystal devices," *IEEE J. Sel. Areas Commun.*, vol. 23, no. 7, pp. 1365–1371, Jul. 2005.
[20] M. Tokushima, H. Yamada, and Y. Arakawa, "1.5-μm-wavelength light guiding in waveguides in square-lattice-of-rod photonic crystal slab," *Appl. Phys. Lett.*, vol. 84, no. 21, pp. 4298–4301, 2004.
[21] J. Bravo-Abad, T. Ochiai, and J. Sánchez-Dehesa, "Anomalous refractive properties of a two-dimensional photonic band-gap," *Phys. Rev. B, Condens. Matter*, vol. 67, no. 11, p. 115116, 2003.
[22] A. Håkansson, J. Sánchez-Dehesa, and L. Sanchis, "Acoustic lens design by genetic algorithms," *Phys. Rev. B, Condens. Matter*, vol. 70, no. 21, p. 214302, 2004.
[23] A. Håkansson, F. Cervera, and J. Sánchez-Dehesa, "Sound focusing by flat acoustic lens without negative refraction," *Appl. Phys. Lett.*, vol. 86, no. 5, p. 054102, 2005.
[24] H. A. Haus, *Wave and Fields in Optoelectronics*. Upper Saddle River, NJ: Prentice-Hall, 1984.

Andreas Håkansson was born in Göteborg, Sweden, in 1976. He received the M.Sc. degree in physical and electrical engineering from the Technical University of Linköping, Linköping, Sweden, in 2002. He has been working toward the Ph.D. degree, first at the Autonomous University of Madrid, Madrid, Spain (2002–2003), and later at the Polytechnic University of Valencia, Valencia, Spain (2003–present).

His research is focused on phononic and photonic crystal device design through optimization.

Pablo Sanchis was born in Valencia, Spain, in 1978. He received the Ingeniero de Telecomunicación (M.Sc.) and Doctor Ingeniero de Telecomunicación (Ph.D.) degrees from the Universidad Politécnica de Valencia, in 2001 and 2005, repectively.

In 2003, he spent a six-month stay in the photonics research group of the Department of Information Technology, Ghent University, Ghent, Belgium. He is Member of the Valencia Nanophotonics Technology Center, Universidad Politécnica de Valencia. His research interests include modeling, design, and fabrication issues in integrated optics, especially in the field of photonic crystals. He has authored or coauthored over 40 papers in peer-reviewed international journals and international conferences.

José Sánchez-Dehesa was born in Toledo, Spain, in 1955. He received the doctoral degree in physics from the Autonomous University of Madrid, Madrid, Spain, in 1982.

From 1985 to 2003, he has been an Associate Professor at the Autonomous University of Madrid. Currently, he is a Full Professor at the Polytechnic University of Valencia, Valencia, Spain, and is the head of the Wave Phenomena Group associated to the Valencia Nanophotonic Technology Center. He has worked on semiconductors and low-dimensional structures such as quantum wells, superlattices, quantum wires, etc. His current work is mainly related with the study of photonic and phononic crystal devices.

Javier Martí (S'89–M'92) received the Ingeniero de Telecomunicación (M.Sc.) degree from the Universidad Politécnica de Catalunya, Catalunya, Spain, in 1991, and the Doctor Ingeniero de Telecomunicación (Ph.D.) degree from the Universidad Politécnica de Valencia, Valencia, Spain, in 1994.

During 1989 and 1990, he was an Assistant Lecturer at the Escuela Universitaria de Vilanova, Barcelona, Spain. From 1991 to 2000, he was a Lecturer and Associate Professor at the Telecommunication Engineering Faculty, where he is currently a Professor and leads the Radio Over Fiber Group. In 2003, he was appointed Director of the Valencia Nanophotonics Technology Center. He has authored or coauthored over 180 papers in referred international technical journals and over 90 papers in international conference proceedings in the fields of broadband hybrid fiber–radio systems and microwave/millimeter-wave photonics, fiber-based access networks, terabit-per-second optical time-division multiplexing (OTDM)/wavlength-division multiplexing (WDM) optical networks, advanced optical processing techniques for microwave signals, and ultra-high-speed data transmission and planar photonic crystals. He is participating very actively in the European Research Framework (FP5 and FP6), leading several projects in the areas of broadband access (OBANET, GANDALF), all-optical processing in photonic networks (LASAGNE), and nanophotonic logic gates (PHOLOGIC).

Prof. Martí has served as a Member of the Technical Program Committee of ECOC, LEOS, Microwave Photonics, and other international workshops and conferences.